Journal of Materials Chemistry B

Accepted Manuscript

ROYAL SOCIETY OF CHEMISTRY

www.rsc.org/materialsB

A Generic Class of Amyloid Fibril Inhibitors

Sian-Yang Ow[1], Innocent Bekard[1], Anton Blencowe[1,2], Greg G. Qiao[1] and Dave E. Dunstan[1*]

[1]*Department of Chemical and Biomolecular Engineering, The University of Melbourne, Victoria 3010, Australia*

[2]*Mawson Institute, Division of ITEE, The University of South Australia, Mawson Lakes, SA 5095, Australia*

**davided@unimelb.edu.au*

Keywords: amyloid fibrils, inhibitors, Amyloid Beta, Bovine Insulin, Lysozyme

ABSTRACT

Amyloid fibrils are large ordered fibrillar aggregates formed from mis-folded proteins. A number of human diseases are linked to the presence of amyloid deposits**,** including Alzheimer's disease, Parkinson's disease and type II diabetes. One therapeutic strategy for treating amyloid related diseases involves inhibiting fibril formation. Amyloid fibrils are β-sheet rich fibrillar aggregates that associate through hydrophobic interactions between precursor units. In this study, these generic physical properties of amyloid fibrils have been exploited to design a universal class of amphiphilic macromolecular inhibitors. A naturally occurring macromolecule of this structure is arabinogalactan protein (AGP), a component of gum arabic (GA). In addition, two synthetic polymers based on the proposed amphiphilic structure were synthesized and tested. These synthetic mimics, referred to as poly(norbornene glucose ester) (PNGE) and poly(norbornene gluconamide) (PNGA), possess hydrophobic polynorbornene backbones and pendent hydrophilic cyclic and open-chain glucose units, respectively. AGP, PNGE and PNGA all show inhibitory effects on *in vitro* amyloid fibril formation in bovine insulin (BI), hen egg white lysozyme (HEWL) and amyloid beta 1-40 (Aβ) proteins. Circular dichroism (CD) spectra of the proteins in the presence of the inhibitors suggests that amyloid fibril formation is inhibited by stabilization of the native α-helices of the proteins, as well as binding of the inhibitors to the β-sheet precursors. Based upon these results, glycosylated hydrophobic macromolecules are identified as a promising class of therapeutic agents for amyloid related diseases. Furthermore, we have determined that the intensity of the fluorescent probe thioflavin T (ThT) is dependent on both fibril morphology and the presence of the inhibitors, and is therefore not a quantitative measure of protein conversion to fibrils.

INTRODUCTION

Amyloid fibrils are fibrillar aggregates of mis-folded proteins with a β-sheet rich structure and a cross-β arrangement.[1] There are currently 15 significant and more than 50 rare human diseases are now known to be associated with amyloid formation.[1, 2] Despite the correlation between disease and the presence of fibrils the role of the amyloid fibrils in disease has not been universally established. The cytotoxic effects associated with amyloidosis have been attributed to the precursors or monomers of the amyloids rather than the mature fibrils.[3] However, there is evidence that fibrils and precursors grown with different shear exposure have varying morphology and degrees of cytotoxicity.[4] The accumulation of the cytotoxic effects from the oligomers and fibrils is believed to result in the amyloid related diseases although the exact causality is still under debate. While it is generally accepted in the literature that ncell cytotoxicity arises from proto-filaments and oligomeric species, we are of the view that the presence of fibrils significantly interrupts transport processes and therefore disrupts physiological function. As such, strategies that inhibit fibril formation are important therapeutic strategies.

One particular therapeutic strategy to tackle amyloid diseases is to inhibit fibril formation and hence the development of inhibitors has been the focus of considerable research effort in recent years.[5] Regland *et al*. and more recently Ritchie *et al*. have shown that treatment with metal chelators can improve the condition of patients suffering from Alzheimer's disease[6] as fibril formation may be facilitated by metal ions. In the mid-1990s the company Elan produced antibodies raised against Aβ, although stage two clinical trials of the antibody failed due to an inflammatory response experienced by several patients.[7] Other methods of preventing amyloid formation that have been studied include using synthetic peptides that bind to fibrils,[8] small ligands to stabilise native Aβ,[9] and targeting of lysine residues that are involved in the self-assembly of the fibril.[10] Ojha et al. have reported the use of polystyrene sulfonate as an amphiphilic polymer which has the capacity to inhibit A-$\beta_{1\text{-}40}$ fibril formation in-vitro.[11]

Here we present a new approach to designing amyloid inhibitors. The key physical attributes of the fibrils and fibril formation mechanism have been used to design a generic class

of inhibitory compounds. The self-assembly of amyloid fibrils occurs at several levels. An initial mis-folding event results in the protein becoming more prone to adopting a β-sheet conformation. The β-sheets that are formed through H-bonding interactions then associate via interactions between the exposed hydrophobic surfaces of the β-sheets.[1, 12] Surfactants that bind to these hydrophobic surfaces have been shown to inhibit amyloid fibril formation.[13] Simple detergent molecules have not been used as therapeutic inhibitors as they are toxic. Therefore, we proposed that an amphiphilic macromolecular structure composed of a hydrophobic backbone with pendent hydrophilic side groups would act as a generic inhibitor of fibril formation. Thus, in the presence of the hydrophobic surface of the β-sheet the macromolecule would adopt a conformation that favours interaction of the hydrophobic backbone with the surface where the hydrophilic side groups then present away from the hydrophobic surface to sterically inhibit further aggregation of the β-sheets (Figure 1a).

Several naturally occurring biopolymers have the generic structural properties required for inhibition of fibril formation as described above, including arabinogalactan proteins (AGPs), a major component of plant gums, such as gum arabic (GA). GA is a common emulsifier in the food industry, and is often used in soft drinks and confectionaries.[14] GA consists of 88.4 wt% polysaccharide arabinogalactan (AG; weight-average molecular weight (M_w) = 380 kDa), 10.4 wt% AGP (M_w = 1.45 MDa), and 1.2 wt% non-AGP glycoprotein (GP; M_w = 250 kDa).[15] The AGP component is responsible for the emulsification capabilities of GA,[14] and is believed to exist as a hybrid between a "wattle blossom" structure and a "twisted hairy rope",[16] with arabinoside and arabinogalactan polysaccharide attachment sites on a hydroxyproline-rich protein sequence.[16, 17] The biopolymer is believed to fold in close proximity with hydrophobic surfaces, such that the hydrophobic protein backbone interacts with hydrophobic surfaces, while the carbohydrate groups remain solvent-exposed.[18] Based upon these characteristics it was hypothesised that AGP would behave as an inhibitor in amyloid fibril formation. Furthermore, the structure of AGP was used as a model to design synthetic mimics that were also synthesised and tested for their inhibitory activity on fibril formation. These amphiphilic synthetic analogues (PNGE and PNGA) were prepared via ring-opening metathesis polymerisation (ROMP) and possess hydrophobic polynorbornene backbones and hydrophilic pendent cyclic and open-chain glucose units (Figure 1b). These compounds are large in molecular weight and would not readily

pass across the blood brain barrier as would be required for in-vivo A-β fibril inhibition. However, we postulate that smaller analogues, particularly glycosylated peptides, present as possible therapeutics.

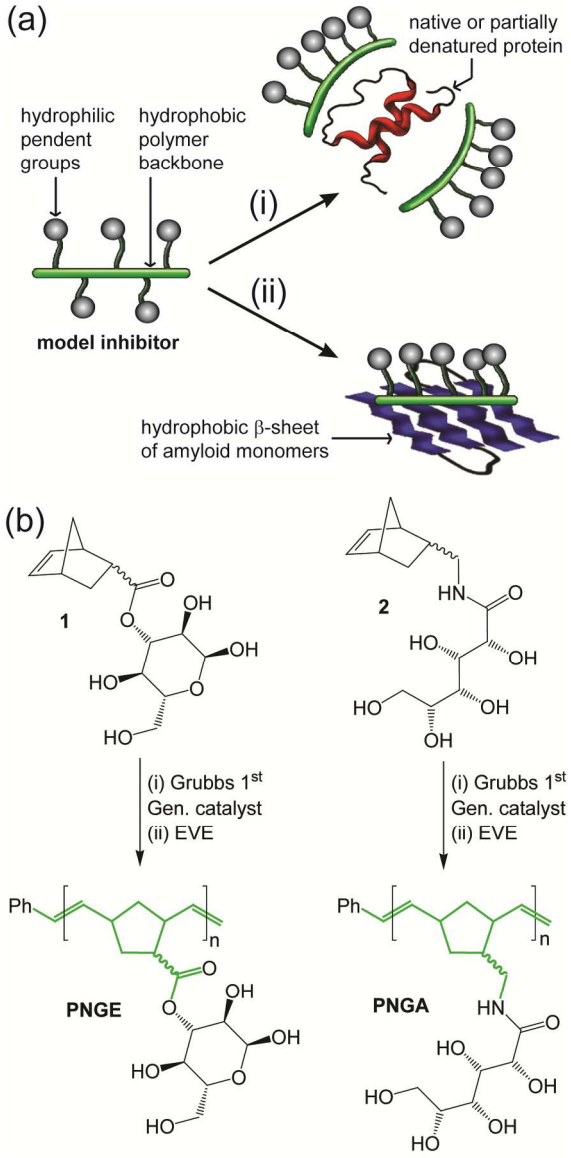

Figure 1: (a) Illustration showing the general structure of the model amphiphilic inhibitors and their proposed binding and inhibitory mechanisms on amyloid fibril formation, involving (i) stabilisation of native, denatured or intermediate protein structures, and (ii) prevention of β-sheet rich amyloid monomers from aggregating and assembling into fibrils. (b) Scheme showing the structures of PNGE and PNGA and their synthesis from the respective monomers **1** and **2** via ROMP.

In this study, the kinetics and morphology of amyloids formed, as well as the potential inhibitory effects of the macromolecular inhibitors (i.e., AGP, PNGE, PNGA and GA), were investigated using three relatively well characterised proteins; bovine insulin (BI), hen egg white lysozyme (HEWL) and amyloid beta 1-40 (Aβ). BI is analogous to human insulin, which forms amyloids that cause abscesses in the insulin injection sites of diabetic patients.[19] Furthermore, insulin amyloid fibril formation is a major limiting factor to the production and storage of insulin.[20] HEWL was used as a model system for human lysozyme, which is implicated in systemic amyloidosis.[21] Aβ was chosen as a model protein system as it is strongly associated Alzheimer's disease.[3] Using the fluorescent probe thioflavin T (ThT) as an indicator of fibril formation both the kinetics and aggregate were determined. ThT is a specific extrinsic dye that fluoresces when bound to amyloid fibrils, with an emission peak at 482 nm when excited at a wavelength of 450 nm.[22] Furthermore, ThT has been shown to not interfere with fibril aggregation,[22] and its fluorescence intensity is proportional to the amount of amyloid formed,[23] barring changes in morphology.[24] Atomic force microscopy (AFM) was used to determine the size and morphology of the aggregates formed in the presence of the inhibitors. CD was employed to study the conformation of the proteins in the presence of the inhibitors and provide insights into the mechanism of inhibition.

EXPERIMENTAL SECTION

Materials

Norbornene-2-carbonitrile (98 %, mixture of *exo* and *endo* isomers), 5-norbornene-2-carboxylic acid (98 %, mixture of *exo* and *endo* isomers), lithium aluminium hydride ($LiAlH_4$, 95 %), gluconolactone, ethyl vinyl ether (EVE, 99 %), anhydrous methanol (99.8 %), 1,2:5,6-di-*O*-isopropylidene-α-D-glucofuranose (diacetone-D-glucose, 98 %), 4-(dimethylamino)pyridine (DMAP, ≥ 99 %), dicyclohexylcarbodiimide (DCC, 98 %), Celite 545, Grubbs 1st generation catalyst (97 %), and trifluoroacetic acid (TFA, 99 %) were purchased from Aldrich and used as received. AR grade dichloromethane (DCM), acetone, ethyl acetate (EtOAc), ethanol (EtOH), methanol (MeOH), diethyl ether (DEE), sodium nitrate ($NaNO_3$) and sodium azide (NaN_3) were purchased from Chem-Supply and used as received. Tetrahydrofuran (THF, RCI Labscan, HPLC grade) was distilled from sodium benzophenone ketyl under argon before use. Deuterated

chloroform ($CDCl_3$, D 99.8 % + 0.03 % v/v TMS), deuterated methanol (CD_3OD, D 99.8 %), and deuterium oxide (D_2O, D 99.9 %) were purchased from Cambridge Isotope Laboratories Inc. and used as received. Ultra high purity argon was purchased from Coregas. High-purity water with a resistivity greater than 18 MΩ·cm was obtained from an in-line Millipore RiOs/Origin water purification system.

Measurements

The molecular weight characteristics of PNGA and PNGE were determined via gel permeation chromatography (GPC) on a Shimadzu liquid chromatography system equipped with a Wyatt DAWN EOS MALLS detector (690 nm, 30 mW) and Wyatt OPTILAB DSP interferometric refractometer (690 nm) using three Waters Ultrahydrogel columns in series ((i) 250 Å porosity, 6 μm diameter bead size; (ii) and (iii) linear, 10 μm diameter bead size) maintained at 50 °C. An aqueous mobile phase containing 50 mM $NaNO_3$ and 0.02 % w/v NaN_3 was used as the eluent at a flow rate of 1 mL/min. Astra software was used to calculate molecular weight values based upon the injected mass. AGP was separated from GA using a Sephacyl gel column. The molecular weight of the purified AGP was measured using GPC and found to be 1.65 x 10^6 g/mol.

^{1}H NMR spectroscopic analysis was performed on a Varian Unity Plus 400 MHz spectrometer using the deuterated solvent as reference.

AFM images were recorded using an MFP3D^t Asylum Research AFM operating in tapping mode. Samples were deposited on freshly peeled mica and dried before imaging. Images of regions covered with the fibrils were recorded to show the morphology of the fibrils. Therefore, the AFM images shown in Figures 3-5 are not quantitative in the mass of fibrils formed as the fibrils were not uniformly deposited on the mica.

Ultracentrifugation was performed using a Beckman Coulter Optima TLX ultracentrifuge with a TLA 100.3 rotor at 65000 RPM (equiv. to 180,000 g) for 1 h at 4 °C. The separation of amyloids from solution was confirmed by the lack of fibrils in the supernatant, as determined by AFM (data not shown).

UV-visible and fluorescence measurements were recorded using a Varian Cary 3E UV-visible Spectrophotometer and Varian Cary Eclipse Fluorescence Spectrophotometer, respectively.

Circular dichroism (CD) readings were performed using a Jasco J-815 or an applied photophysics Chirascan Plus CD instrument. Dichroweb^{tm} Circular Dichroism web-based deconvolution software was used for the deconvolution of the CD spectra.[25]

Procedures

Preparation of Protein and Inhibitor Solutions. Purified protein samples BI and HEWL were obtained from Sigma Aldrich and Aβ from Keck Laboratories, Yale University. Stock solutions of each protein were prepared as follows. BI and HEWL were dissolved separately in filtered 0.1 % HCl solutions at pH 1.5. Aβ was dissolved in a filtered 20 μM NaOH solution (260 μL) and sonicated for 15 min in an iced sonic bath before the addition of 64.6 mM phosphate buffer solution (PB; pH 7.5, 1040 μL) and centrifugation at 20000 g for 5 min. The protein concentrations in the stock solution were measured via UV-vis spectrophotometry using previously reported extinction coefficients: 5730 $M^{-1}cm^{-1}$ at 280 nm[26] for BI; 37895 $M^{-1}cm^{-1}$ at 280 nm[27] for HEWL; and 55771 $M^{-1}cm^{-1}$ at 214 nm for Aβ.[28] The concentration of the stock solutions were adjusted using either 0.1 % HCl (for BI and HEWL) or PB (for Aβ) to provide final solutions containing 0.2 mg/mL of protein, 50 μM thioflavin T (ThT; Sigma) and either 0.2 or 2 mg/mL of the macromolecular inhibitors.

Isolation of AGP. AGP was purified from GA (Sigma Aldrich) by centrifuging a 200 mg/mL GA solution, followed by a two stage precipitation using Na_2SO_4, as previously described by Anderson *et al* .[29] Precipitates were dialysed and dried, then dissolved in 0.5 M NaCl and fractionated via size exclusion chromatography using Waters Ultrahydrogel columns (500 and 2500 Å porosity in series) for microgram quantities or a Sephacryl^{TM} 400 column for milligram quantities. AGP purity was verified using GPC; a single peak was observed on all detectors with an estimated M_w value of 1.65 MDa. The GPC traces (Supporting Information (SI), Figures S1-4) were similar to those previously reported in the literature.[16, 30]

Synthesis of Poly(norbornene glucose ester) (PNGE). 3-*O*-(5-Norbornene-2-carboxy)-D-glucose **1** (237 mg, 0.79 mmol) was dissolved in a solution of MeOH (960 µL)/water (330 µL) under argon in a vial fitted with stirrer bar and sealed with a Suba seal. Separately, Grubbs 1st generation catalyst (32.0 mg, 38.8 µmol) was dissolved in DCM (6.3 mL) under argon and added to the mixture with rapid stirring. After 30 min, a solution of MeOH (5.0 mL)/water (1.7 mL) was added and the mixture was stirred at room temperature for 2 h. EVE (2 mL) was added and the mixture was stirred for a further 2 h before being concentrated *in vacuo* (0.5 mbar). The residue was dissolved in water (20 mL), extracted with chloroform (5 × 10 mL), concentrated *in vacuo* (0.5 mbar), redissolved in MeOH (3 mL), and precipitated into acetone (40 mL). The precipitate was isolated via centrifugation (2000 g), redissolved in MeOH (3 mL) and then precipitated again into acetone (40 mL). This step was repeated three times in total and the isolated precipitate was dried *in vacuo* (0.1 mbar) to afford the polymer as a pale brown solid, 28 mg. ^{1}H NMR (CD_3OD, 400 MHz) δ_H 1.50 (*br s*), 1.71-1.94 (*m*), 2.16 (*br s*), 2.58-2.65 (*m*), 2.85 (*br s*), 3.00 (*br s*), 3.24-3.37 (*m*), 3.48-3.52 (*m*), 3.67-3.87 (*m*), 4.56 (*br s*), 4.81-4.96 (*m*), 5.11-5.30 (*m*), 5.35-5.58 (*m*), 6.17-6.31 (*m*, end-group), 6.39-6.50 (*m*, end-group), 7.15-7.40 (*m*, end-group) ppm; M_n (NMR) 1.8 kDa. GPC (aq.) M_n 1.5 kDa; PDI = 1.16.

Synthesis of Poly(norbornene gluconamide) (PNGA). *N*-((Bicyclo[2.2.1]hept-5-en-2-yl)methyl)-2,3,4,5,6-pentahydroxyhexanamide **2** (101 mg, 336 µmol) was dissolved in a solution of MeOH (400 µL)/water (130 µL) under argon in a vial fitted with stirrer bar and sealed with a Suba seal. Separately, Grubbs 1st generation catalyst (13.7 mg, 16.7 µmol) was dissolved in DCM (2.5 mL) under argon and added to the mixture with rapid stirring. After 30 min, a solution of MeOH (2.1 mL)/water (0.7 mL) was added and the mixture was stirred at room temperature for 12 h. EVE (2 mL) was added and the mixture was stirred for a further 2 h before being transferred to a centrifuge tube containing DCM (10 mL) and water (25 mL). The mixture was vortexed, centrifuged (2000 g) and the organic phase was separated. The aqueous phase was washed with EtOAc (2 × 10 mL), concentrated *in vacuo* (20 mbar) to *ca.* 2 mL, and precipitated into acetone (40 mL). The precipitate was isolated via centrifugation (2000 g) and dried *in vacuo* (0.1 mbar) to afford the polymer as a pale brown crystalline solid, 37 mg. ^{1}H NMR (D_2O, 400 MHz) δ_H 1.72 (*br s*), 3.00 (*br s*), 3.50-3.63 (*m*), 3.92 (*br s*), 4.13 (*br s*), 5.28 (*br s*), 7.20 (*br s*, end-group) ppm; M_n (NMR) 4.7 kDa. GPC (aq.) M_n 6.8 kDa; PDI = 1.09.

Fibril Formation: Protein/ThT dye solutions with or without inhibitors were incubated in a fluorescence spectrophotometer with constant stirring: 550 RPM at 60 °C for BI; 840 RPM at 70 °C for HEWL; and 550 RPM at 37 °C for Aβ. A single cell peltier was used for BI while a multi-cell holder was used for Aβ and HEWL. ThT fluorescence was measured at 5 min intervals with an excitation wavelength of 450 nm and the emission intensity was measured at 482 nm. Control measurements with GA and ThT showed very little fluorescence (I~5-10a.u.) Addition of GA during fibril incubation (data not shown) showed no increase in ThT fluorescence indicating that the GA inhibitor resulted in no increase in biding sites for the ThT. Repeats of the control measurements of the kinetic traces (absence of inhibitors) showed variation of approximately 20% in the plateau intensity values.

Determination of Amyloid Content. Incubated protein solutions were centrifuged (180,000 g) for 1 h at 4 °C and the supernatants were analysed via UV-vis spectrophotometry to determine the concentration of protein not converted to fibrils. The adjusted absorbance was calculated by subtracting the calculated ThT absorbance contribution from the absorbance value at the measured wavelength (280 nm for BI and HEWL and 214 nm for Aβ). The ThT concentration was determined using the absorbance of the sample at 450 nm, with reference to calibration plots recorded in identical solvents (0.1% HCl, pH 1.5 for BI and HEWL, phosphate buffer for Aβ) as the protein samples to compensate for any pH effects on the ThT (data not shown). The measured absorbance of the ThT at 450nm was not corrected for scattering as the absorbance was significantly larger than the baseline scattering in the spectra. The percentage of protein converted to amyloid was calculated from the difference in adjusted absorbance at 280nm before and after ultracentrifugation.

RESULTS AND DISCUSSION

Preparation of Macromolecular Inhibitors

Purified AGP was isolated from GA via a combination of precipitation using Na_2SO_4,[29] dialysis and size exclusion chromatography, as previously reported in the literature.[19,32] Isolation

of AGP was verified via GPC using light scattering, differential refractive index (DRI) and UV-visible detectors.[19,32] Whereas the DRI chromatogram of GA consists of a unsymmetrical broad peak with a shoulder to low retention time, the UV chromatogram at λ = 206 nm displayed a peak with a maxima aligned with the shoulder in the DRI chromatogram (SI, Figure S1), which is characteristic of the higher absorbance of the peptide backbone in AGP. Following separation, the DRI, UV and light scattering chromatograms revealed a narrower symmetrical distribution at lower retention time with a M_w of 1.65 × 10^6 Da (SI, Figure S2-4), which is consistent with that previously reported for AGP.[18]

PNGE and PNGA were prepared via ROMP of the monosaccharide norbornene monomers **1** and **2** (refer to SI for details and Figures S5 and 6, respectively), respectively, using the 1st generation Grubbs catalyst. The monomers (and polymers) were designed with cyclic and linear glucose groups so that the effect of this structural parameter on the activity of the inhibitor could be studied. ROMP was conducted in a mixed dichloromethane, methanol and water solvent system with the intermittent addition of more methanol and water to improve the initial solubility of the catalyst and prevent precipitation of the polymers at higher monomer conversions. Subsequently, the catalyst was removed from the terminal of the polymer chains via the addition of ethyl vinyl ether (EVE) to afford PNGE and PNGA with polynorbornene backbones and pendent glucose groups. ^{1}H NMR spectroscopic analysis of the polymers (Figure 2) revealed resonances consist with the polynorbornene backbone, pendent glucose groups and phenyl end-groups derived from the catalyst/initiator. For both PNGE and PNGA, resonances resulting from the vinyl groups along the polymer backbone and pendent glucose units were observed between *ca.* δ_H 5.0-5.5 and 3.5-4.0 ppm, respectively (Figure 2, resonances a and d, respectively). In addition, resonances resulting from the phenyl end-groups of the polymers were present at *ca.* δ_H 7.2 ppm (Figure 2, resonances e), which enabled determination of the number-average molecular weight (M_n) values of 1.8 and 4.7 kDa for PNGE and PNGA, respectively. These results are consistent with the GPC data for PNGE and PNGA, which yielded M_n values of 1.5 (polydispersity (PDI) = 1.16) and 6.8 (PDI = 1.09) kDa. The higher molecular weight of PNGA was attributed to the longer polymerisation time used during its synthesis, relative to PNGE.

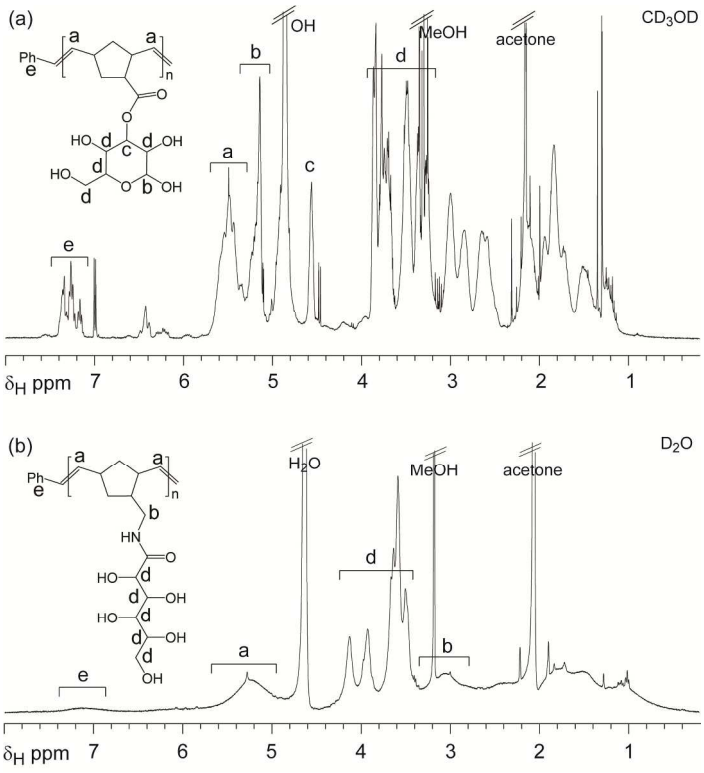

Figure 2: ^{1}H NMR spectra of (a) PNGE and (b) PNGA in CD_3OD and D_2O, respectively.

Fibril Formation

Several commonly used measurements of fibril formation *in vitro include*[3] fibril specific dyes, light scattering, centrifugation, CD, and Raman and FTIR spectroscopic methods.[31] Typical kinetic curves associated with amyloid fibril formation are reported here using ThT fluorescence, which is generally accepted as a measure of fibril formation.[32] The ThT fluorescence results are supported using both ultracentrifugation and AFM imaging. Characterisation of the fibril morphology was undertaken using AFM after fibril formation had run to completion. Ultracentrifugation of the incubated solutions was conducted in order to determine the conversion of protein to fibrils.

There are a wide range of proteins for which *in vitro* testing of fibril formation has been conducted in order to examine the mechanisms and parameters that influence amyloid formation.[33] Most *in vitro* tests have been performed in solutions that differ significantly from

physiological temperatures, pH values and salt concentrations to allow fibril formation within reasonable laboratory time frames. Typical *in vivo* fibril formation is thought to occur over years under normal physiological conditions.[34] In this study, bovine insulin (BI),[23,34] hen egg white lysozyme (HEWL)[25] and amyloid beta 1-40 (Aβ)[2] were employed as their conversion to fibrillar aggregates has been well characterised.

Bovine Insulin (BI). BI was incubated in the presence of GA, AGP, PNGA and PNGE at 2 mg/mL, for which the resulting fluorescence and fibrillar morphologies are presented in Figure 3. BI incubated alone without inhibitors resulted in a plateau intensity of *ca.* 150 A.U and lag time of *ca.* 7 h, with the formation of long thin fibrils (Figure 3b). The addition of 2 mg/mL GA and AGP to the BI solutions resulted in increased final plateau fluorescence intensities, but increased the lag time (> 15 h) of the fibril formation (Figure 3a). The high plateau ThT fluorescence intensities suggest larger amounts of fibril formation, however, the mass balance results obtained from ultracentrifugation (Table 1) indicate less fibrils were produced. The ultracentrifugation experiments show the protein conversion to fibrils, and are therefore a measure of the efficacy of the inhibitors. AFM imaging revealed that the fibril morphology is modified to form large rope like structures in the presence of GA and AGP (Figures 3c and d, respectively). While it can be seen that the AGHP and GA also cause the formation of large rope like structures, a number of smaller fibrils are also present. These results imply that ThT is not always a quantitative measure of fibril mass. The control with no inhibitor (94 % conversion) shows a significantly lower final ThT intensity than both GA and AGP, which show lower conversion to fibrils (82 and 87 %, respectively) than the control (Figure 3a). It has generally been assumed in the literature that ThT intensity is proportional to the fibril mass produced.[35] Rather the ThT fluorescence is dependent upon the fibril morphology and possibly the presence of the inhibitor. We postulate that the AGP is binding to the fibrils to create an increase in ThT binding sites for a similar mass of material.[36] Unfortunately, the GA and AGP concentration remaining in solution after centrifugation was not determined. While GA and AGP show small overall effects on the mass of fibrils formed, they significantly increase the lag time associated with fibril formation. This suggests that the AGP (also found in GA) is associating with the BI protein to stabilise it and increase the lag time of fibril formation.

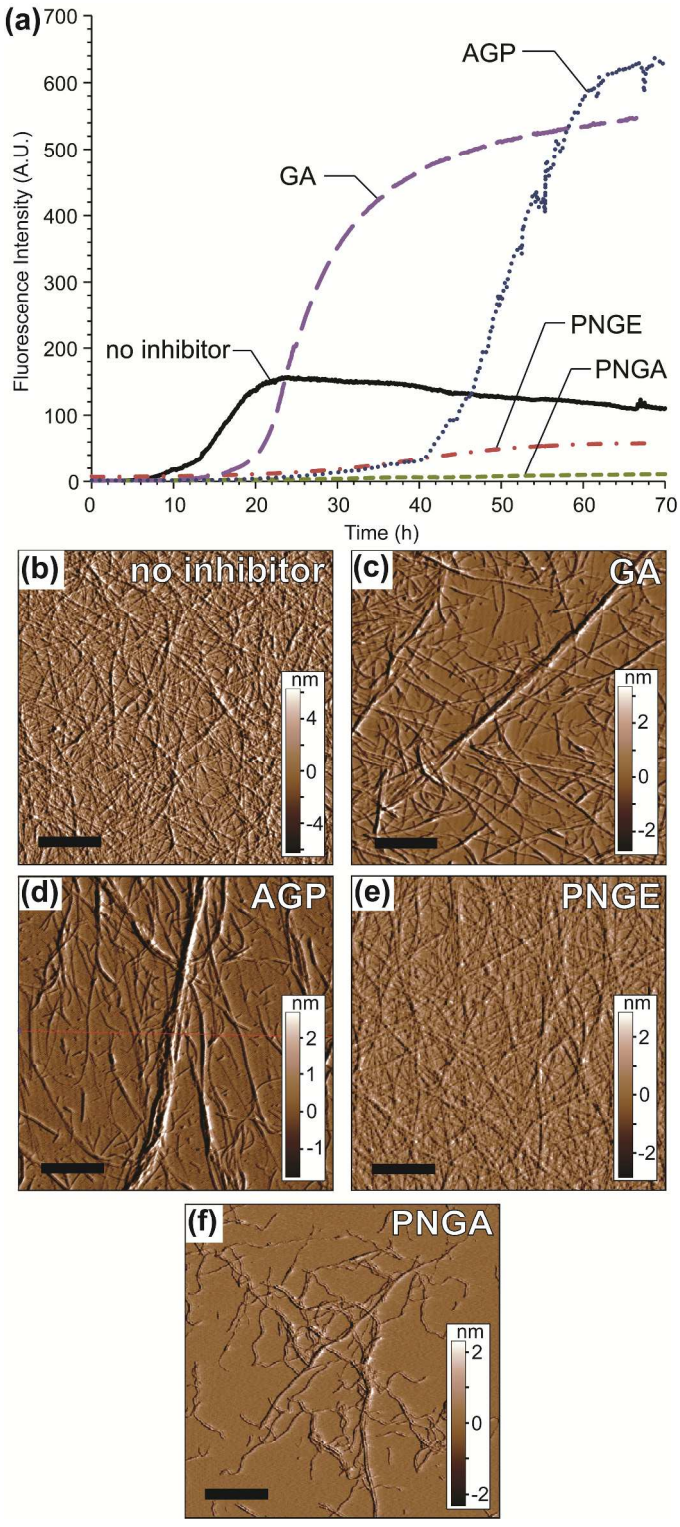

Figure 3: (a) Fluorescence intensity over time for BI incubated with and without the inhibitors. AFM amplitude images showing BI fibrils formed in the (b) absence of inhibitors, and with 2 mg/mL (c) GA, (d) AGP, (e) PNGE and (f) PNGA. All AFM images are 10 μm^2 with 2 μm scale bars. The AFM images were taken after completion of the kinetic traces.

In comparison, the synthetic inhibitors PNGE and PNGA significantly reduced the ThT fluorescence intensity and greatly increased the lag time of BI fibril formation (Figure 3a). Fibrils formed in the presence of PNGE (Figure 3e) possessed a similar morphology to those grown without inhibitor (Figure 3b). However, BI amyloid fibrils formed in the presence of PNGA (Figure 3f) appeared to be much shorter than those formed without inhibitor (Figure 3b). Furthermore, both PNGE and PNGA significantly reduced the conversion of protein to fibrils (Table 1), consistent with the reduced final ThT intensities observed (Figure 3a).

To investigate the conformational changes in the proteins and assess the possible mechanism of inhibition of the inhibitors, CD spectra of the inhibitors (SI, Figures S7-9), native BI (SI, Figures S10) and fibrils formed in the presence of the inhibitors (SI, Figures S11-12) were recorded. Deconvolution of the CD spectra of the inhibitors alone revealed no specific conformations, with the macromolecular inhibitors adopting random coil conformations. In contrast, the CD spectra of native BI and BI incubated with the inhibitors revealed an α-helical to β-sheet conversion during the fibril formation in all samples except for BI incubated with PNGA, which retained a relatively high 43 % α-helical content (SI, Figures S10-12 and Table S1). These results suggest that PNGA preserves the native α-helical structure of BI, inhibiting unfolding and fibril formation.

Hen Egg White Lysozyme (HEWL). HEWL was incubated in the presence of 2 mg/mL GA and AGP, and 0.2 mg/mL PNGA and PNGE. Fluorescence intensity versus time and the fibrillar morphologies obtained for inhibition tests with 0.2 mg/ml of HEWL are shown in Figure 4. The HEWL fibrils that were formed (Figure 4a-f) are notably shorter than the BI amyloid fibrils (Figure 3b-f). The results of ultracentrifugation of the HEWL amyloids grown with and without the inhibitors are presented in Table 1.

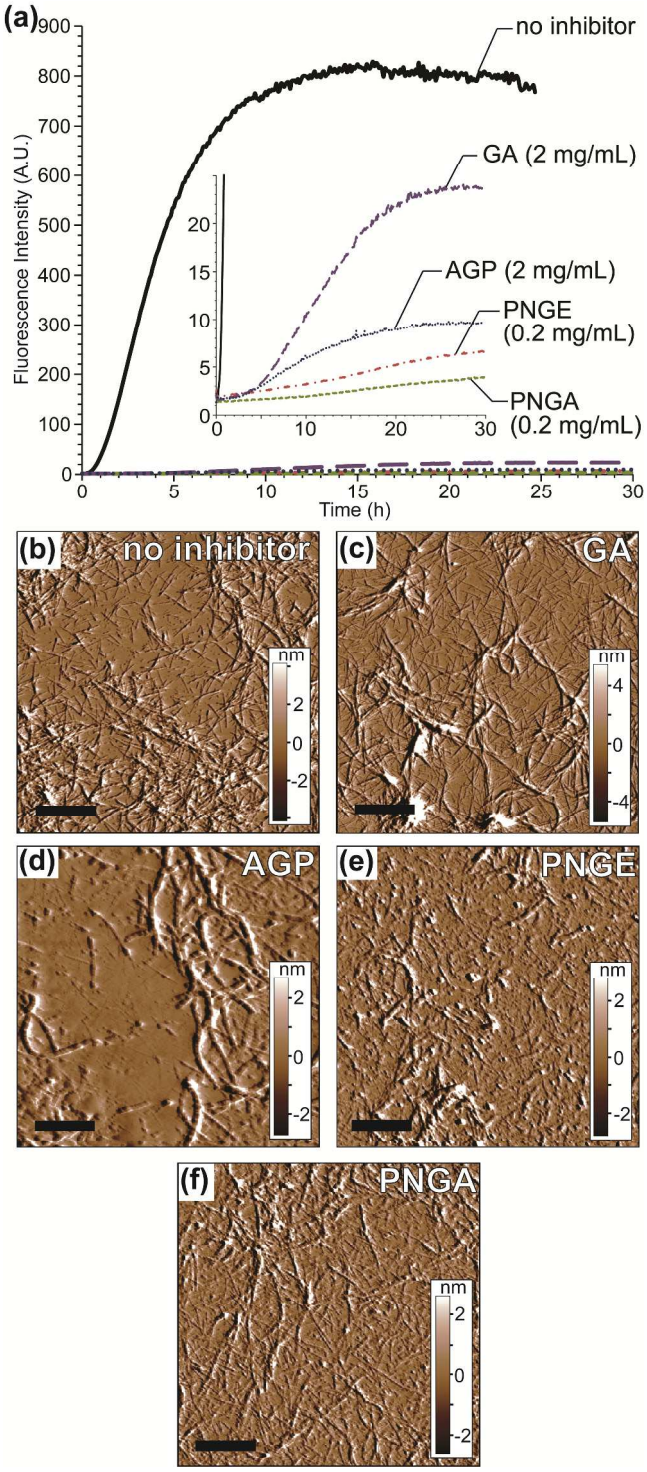

Figure 4: (a) Fluorescence intensity over time for HEWL incubated with and without the inhibitors; inset is expansion of the fluorescence intensity region over 0-25 A.U. AFM amplitude images showing HEWL fibrils formed in the (b) absence of inhibitors, and with 2 mg/mL (c) GA and (d) AGP, and 0.2 mg/mL (e) PNGE and (f) PNGA. All AFM images are 10 μm^2 with 2 μm scale bars. The AFM images were taken after completion of the kinetic traces.

All inhibitors tested with HEWL were effective at inhibiting fibril formation as measured by ThT as observed in a significant reduction of fluorescence intensity and increased lag time from < 1 h for the HEWL control to *ca.* 5 h in the presence of the inhibitors (Figure 4a). This observation was supported by the measured reduction in protein to fibril conversion for all the inhibitors tested using centrifugation (Table 1). PNGA displayed the strongest inhibitory effects at a concentration of 0.2 mg/mL as seen in the ThT fluorescence (Figure 4a) and ultracentrifugation experiments (Table 1). AFM images of HEWL fibrils formed in the presence of GA and AGP revealed large intertwined rope-like aggregates (Figure 4c and d, respectively). Larger fibrils were also observed for BI in the presence of GA and AGP suggesting that their effect on both HEWL and BI fibrils is similar. In contrast to BI (Figure 3a), the fluorescence intensity of HEWL with GA and AGP was lower than that of HEWL without inhibitor (Figure 4a). Both AGP and GA significantly reduced the conversion of HEWL to fibrils by a factor of *ca.* 3 (Table 1), which may offset any increase in ThT fluorescence conferred by the large HEWL fibrils (Figures 4c and d). HEWL fibrils formed in the presence of PNGE and PNGA (Figures 4e and f, respectively) had a similar morphology to native fibrils (Figure 4b). Similar to the CD results obtained for BI, HEWL incubated with and without the inhibitors revealed an α-helical to β-sheet conversion during the fibril formation in all samples (SI, Figures S13-14 and Table S2). A slight decrease in the β-sheet content was observed in the presence of all the inhibitors, with PNGA once again displaying the highest α-helical content.

Amyloid Beta (Aβ). When incubated in the absence of inhibitors Aβ rapidly formed amyloid fibrils with a lag time of *ca.* 15 min and a plateau fluorescence intensity of *ca.* 325 A.U (Figure 5a). AFM images of A-β incubated in the absence of inhibitors revealed many short amyloid fibrils that aggregate into large masses as seen in the top right of Figure 5b). In the presence of the inhibitors a reduction in the resulting fluorescence was observed (Figure 5a). Furthermore, the ultracentrifugation experiments revealed that all inhibitors caused a reduction in fibril yield relative to incubation with no inhibitor (Table 1).

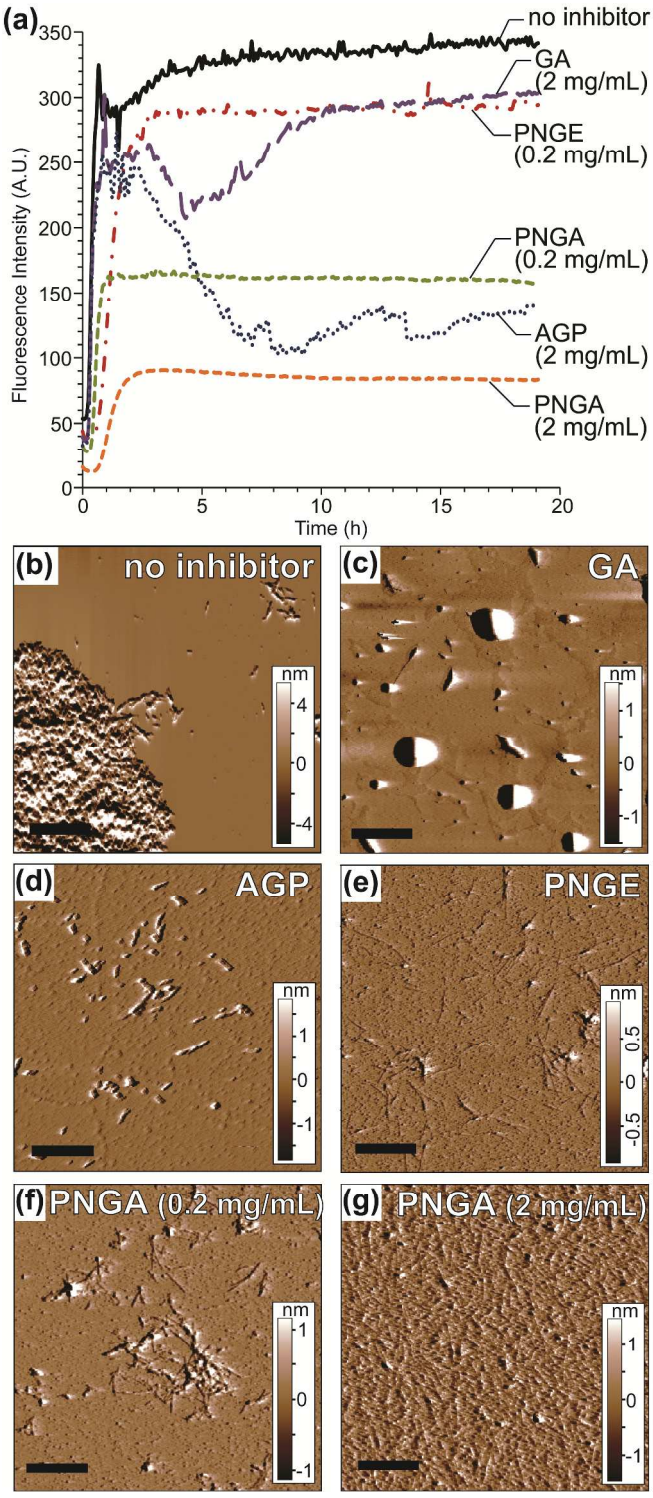

Figure 5: (a) Fluorescence intensity over time for Aβ incubated with and without the inhibitors. AFM amplitude images showing Aβ fibrils formed in the (b) absence of inhibitors, and with 2 mg/mL (c) GA, (d) AGP and (e) PNGE, and (f) 0.2 mg/mL PNGA and (g) 2 mg/mL PNGA. All AFM images are 10 μm^2 with 2 μm scale bars. The AFM images were taken after completion of the kinetic traces. Regions of flocculated fibrils were observed using the AFM. These regions are not shown in images d-g. The images are of selected regions where no aggregates were found in order to show the size and morphology of the individual fibrils.

Aβ fibril formation showed only minor inhibition with GA and AGP, with little associated change in the lag time and a small (50 A.U) reduction in the peak fluorescence intensity (Figure 5a). When Aβ was incubated with GA or AGP the fluorescence intensity decreased after the peak at around 2 h, which is attributed to GA and AGP causing flocculation of Aβ fibrils that floated above the excitation light beam of the fluorimeter. Additionally, flocculation of the fibrils is believed to be responsible for the high amount of noise (Figure 5a) caused by the heterogeneous nature of the flocculated mixture. Although the peak ThT fluorescence intensities of Aβ incubated with GA and AGP appear similar, it was difficult to determine the peak fluorescence intensity due to the flocculation of the fibrils. Ultracentrifugation experiments (Table 1) revealed that at the same concentration AGP was a more effective inhibitor than GA (89 and 59 % conversion to amyloid fibrils, respectively), further supporting the theory that AGP is the primary amyloid inhibitory component of GA.

Incubation with 0.2 mg/mL of PNGA and PNGE appeared to cause some inhibition of Aβ amyloid fibril formation. Whereas 0.2 mg/mL of PNGE increased the lag time of Aβ amyloid formation from 15 min to 60 min and reduced the plateau fluorescence intensity slightly, 0.2 mg/mL of PNGA caused a slight increase in the lag time but a greater reduction in the plateau fluorescence intensity to *ca.* 160 A.U (Figure 5a). When 2 mg/mL of PNGA was employed a further reduction in the peak fluorescence to 80 A.U was observed, with an increased lag time to *ca.* 60 min (Figure 5a). These results are indicative of a concentration dependent inhibitory effect as would be expected. Ultracentrifugation experiments (Table 1) imply that the reduction in fluorescence intensity results from a reduction in the conversion of protein to fibrils. Based upon these observations PNGA is a more potent inhibitor than PNGE and both of these macromolecules are more effective at inhibiting amyloid fibril formation of Aβ than GA and AGP. This is consistent with observations from the similar experiments conducted with BI and HEWL (Figure 3 and 4, respectively).

AFM imaging of the Aβ fibrils grown with GA showed the presence of small fibrils, large round non-fibrillar aggregates as well as a mat of proteinaceous material on the mica (Figure 5c). Small fibrils can be seen between the large spherical aggregates. Aβ fibrils produced in the presence of AGP (Figure 5d) appeared to be similar to those produced with 0.2 mg/ml PNGE

and PNGA (Figure 5e and 5f), and consisted of a mixture of short fibrils with a large number of non-fibrillar aggregates. The CD spectra of the aggregates formed in the presence of 2 mg/mL of GA, AGP and PNGA revealed an increased amount of α-helical structures (42-48 %) relative to Aβ fibrils formed in the absence of inhibitors (12 %) (SI, Figures S15-16 and Table S3). These results imply that the non-fibrillar proteinaceous masses observed for 2 mg/mL of GA, AGP and PNGA were largely made of Aβ that folded into an alternate α-helical rich conformations, suggesting that the inhibition of amyloid fibril formation occurred by locking Aβ into alternative, non-fibrillar conformations, thus preventing β-sheet rich monomer formation.

Ultracentrifugation experiments revealed that all of the inhibitors reduced the amount of fibril formation in the three protein systems investigated (Table 1), although their effects varied for each protein. From the ultracentrifugation data, PNGA caused the greatest reduction in protein conversion to fibrils, which is consistent with ThT fluorescence data (Figures 3-5). There is a strong argument that PNGA was the most effective amyloid inhibitor of the four tested in this study. Furthermore, the general reduction of amyloid conversion (Table 1) implies that amphiphilic macromolecular inhibitors can be effective universal amyloid inhibitors, as they were able to inhibit amyloid fibril formation in three unrelated amyloid-forming protein systems.

Table 1: Percentage conversion of the proteins to fibrils as measured from ultracentrifugation experiments.

Inhibitor	Concentration (mg/mL)	BI % Conversion to amyloid[a]	HEWL % Conversion to amyloid[a]	Aβ % Conversion to amyloid[a]
No inhibitor	N/A	94	41	100[b]
GA	2	82	15	89
AGP	2	87	12	59
PNGE	2	29	[c]	[c]
	0.2	[c]	31	72
PNGA	2	15	[c]	31
	0.2	[c]	15	[c]

[a] Absorbance values of the solution and supernatant (λ = 280 nm for BI and HEWL, and λ = 214 nm for Aβ) were converted to protein concentration and the conversion to fibrils determined by the difference. [b] The percentage conversion to amyloid value for Aβ with no additive is assumed to be at 100% due to the extremely low absorbance of the supernatant. [c] Not measured. All values of % conversion have an error of +/-20% of the quoted value.

Differences in Inhibitory Effects.

It is believed that PNGE and PNGA were more effective inhibitors than AGP for several reasons. Firstly, PNGE and PNGA have larger hydrophobic repeat units in their polymer backbone, which contributes to an overall increase in the percentage of hydrophobic components versus hydrophilic components and may improve their interaction with the hydrophobic surfaces of protein structures. Secondly, the carbohydrate side chains of AGP may have been excessively large and thus hindered inhibition of amyloid fibril self-assembly due to steric effects. The AGP has been generally described as having a "wattle blossom structure" where the polysaccharide groups are pendant to the protein backbone. See Figure 1a. for the general structure which is also shown in the work by Randall et al.[15]In comparison, PNGE and PNGA have significantly smaller pendent monosaccharide groups. Thirdly, the difference in molecular weight of AGP, PNGA and PNGE (M_w = 1.45 MDa, 1.7 kDa and 7.4 kDa, respectively), and possibly molar concentration, may account for the observed differences in inhibitory activity. This suggests that a smaller molecular weight amphiphilic macromolecule may be a more effective inhibitor for similar mass concentrations, although it is not possible to decouple the effects of molecular weight and molar concentration between AGP and the synthetic inhibitors in the current study. The investigation of such effects is the topic of ongoing studies. However, for PNGE and PNGA, where the total hydrophobic backbone surface areas are very similar for the same 2 mg/mL concentration (given that the repeat units have a very similar molecular weight), the improved inhibitory activity of PNGA would imply that the open-chained structure of the pendent glucose groups acts as a better hydrophilic stabilizing group compared to the cyclic glucose structure of PNGE.

It was also observed that Aβ fibril formation was least affected by the inhibitors when compared to BI or HEWL. A possible reason for this may be that Aβ is found in a random chain structure rather than containing α-helices. It is also the least stable of the three proteins as a consequence of its natively disordered structure (SI, Figure S13) and has the ability to form amyloid fibrils spontaneously under physiological conditions. HEWL is the most stable of the three proteins due its relatively large size, the larger amount of intramolecular bonding and that higher incubation temperatures (70 °C) are required for amyloid formation. Hence, Aβ fibril

formation would be more difficult to prevent than BI or HEWL amyloid formation, resulting in weaker observed inhibitory effects of the compounds investigated. Alternatively, this may also result from the lower molecular weight of Aβ (1450 Da) as compared to BI (5734 Da) or HEWL (37895 Da). Hence, with a lower molecular weight, Aβ has the highest molar concentration for 0.2 mg/mL and therefore, the molar ratio of inhibitor to protein would be lower. For the 0.2mg/ml inhibitor concentrations the molar ratios of the inhibitors are significantly different. For AGP the ratio of inhibitor to protein (I/P) is $9X10^{-4}$, $3.5x10^{-3}$, $2.3x10^{-2}$ for the A-β, BI and HEWL respectively. Given the range of ratios of the I/P, there appears to be a consistent trend for the AGP with molar ratio and inhibitor efficiency. The I/P ratio for PNGE for the three proteins is 0.8, 1.2 and 21 for A-β, BI and HEWL respectively while for PNGA the ratios are 0.3, 1.2 and 8 in the same order. (These values are for 0.2mg/ml. The values at 2.0mg/ml are 10 times higher). The trend in inhibitory efficiency for the PNGA and PNGE is consistent with the molar ratios however the AGP shows the most effective inhibitory activity based on this ratio.

Finally, it is also possible that the difference in inhibitory effect between the three proteins results from the structure of the proteins themselves. Aβ in the incubation conditions used adopts a natively disordered (random coil) structure, while BI and HEWL were both largely α-helical (refer to SI, Tables S1-S3). It is possible that the inhibitors used may have a preference for stabilising α-helical structures or that the inhibitors were less capable of binding as strongly to the hydrophobic surfaces presented on the Aβ amyloid monomers compared to those of BI or HEWL. Therefore, the structure of Aβ or the differences in incubation conditions may play a role. As a result, the inhibition of Aβ fibril formation by these the macromolecular inhibitors was not as pronounced as the observed inhibition of BI and HEWL fibril formation.

CONCLUSIONS

By using the generic properties of amyloid fibril self-assembly, it is proposed that an amphiphilic macromolecular inhibitor with a generic structure consisting of hydrophobic backbone and hydrophilic side chains can inhibit amyloid fibril formation. In support of this theory, GA, AGP, PNGA and PNGE were shown to inhibit the formation of amyloid fibrils with the proteins BI, HEWL and Aβ *in vitro*. It is proposed that these inhibitors preserve the native or intermediate α-helical structures for BI and HEWL while stabilizing the intermediate α-helical

structure in A-β. Furthermore, we postulate that the inhibitors bind to exposed hydrophobic surfaces of the amyloid monomers, which renders them water soluble, and ultimately prevents amyloid fibril formation. This study demonstrates that amphiphilic polymers are effective amyloid inhibitors that are capable of inhibiting amyloid growth for three distinctly different proteins. The proposed chemical structure can be used as a template for a new class of amyloid inhibitors with the potential to effectively combat amyloid fibril diseases. Furthermore, the use of ThT as a quantitative tool in measuring amyloid fibril formation was shown to be problematic for inhibition testing as the fibril morphology and/or the presence of the inhibitors has a pronounced effect on the observed fluorescence intensities.

ACKNOWLEDGEMENTS

We would like to thank Kevin Barnham and John Gehman from the Bio21 Institute for use of the circular dichroism instrument.

SUPPORTING INFORMATION

GPC DRI, LS and UV chromatograms for the separation of AGP from GA, procedures for the synthesis of monomers **1** and **2**, ^{1}H NMR spectra for monomers **1** and **2** and their precursors, and CD spectra and conformational analysis of the proteins in the presence of the macromolecular inhibitors.

REFERENCES

[1] M. Fändrich, Cellular and Molecular Life Sciences 2007, 64, 2066
[2] F. Chiti, C. M. Dobson, Annual Review of Biochemistry 2006, 75, 333.
[3] M. Stefani, Biochimica et Biophysica Acta 2004, 1739, 5
[4] S. Lee, E. J. Fernandez, T. A. Good, Protein Science 2007, 16, 723
[5] H.-W. Klafki, M. Staufenbiel, J. Kornhuber, J. Wiltfang, Brain 2006, 129, 2840; I. Melnikova, Nature Reviews 2007, 6, 341.

[6] C. W. Ritchie, A. I. Bush, A. Mackinnon, S. Macfarlane, M. Mastwyk, L. MacGregor, L. Kiers, R. Cherny, Q.-X. Li, A. Tammer, D. Carrington, C. Mavros, I. Volitakis, M. Xilinas, D. Ames, S. Davis, K. Beyreuther, R. E. Tanzi, C. L. Masters, Archives of Neurology 2003, 60, 1685 ; B. Regland, W. Lehmann, I. Abedini, K. Blennow, M. Jonsson, I. Karlsson, M. Sjögren, A. Wallin, M. Xilinas, C.-G. Gottfries, Dementia and Geriatric Cognitive Disorders 2001, 12, 408

[7] J. A. R. Nicoll, D. Wilkinson, C. Holmes, P. Steart, H. Markham, R. O. Weller, Nature Medicine 2003, 9, 448

[8] W. Höyer, C. Gronwall, A. Jonsson, S. Ståhl, T. Härd, Proceedings of the National Academy of Sciences 2008, 105, 5099

[9] C. Nereliusa, A. Sandegren, H. Sargsyan, R. Raunak, H. Leijonmarck, U. Chatterjee, A. Fisahn, S. Imarisio, D. A. Lomas, D. C. Crowther, R. S. mberg, J. Johansson, Proceedings of the National Academy of Sciences 2009, 106, 9191 ; I. W. Hamley, Chemical Reviews 2012, 112, 5147.

[10] S. Sinha, D. H. J. Lopes, Z. Du, E. S. Pang, A. Shanmugam, A. Lomakin, P. Talbiersky, A. Tennstaed, O. K. McDaniel, R. Bakshi, P.-Y. Kuo, M. Ehrmann, O. G. B. Benedek, J. A. Loo, F.-G. Klarner, T. Schrader, C. Wang, G. Bitan, Journal of the American Chemical Society 2011, 133, 16958

[11] B. Ojha, H. Liu, S. Dutta, P. P. N. Rao, E. P. Wojcikiewicz, D. Du, The Journal of Physical Chemistry B 2013, 117, 13975.

[12] O. S. Makin, E. Atkins, P. Sikorski, J. Johansson, L. C. Serpell, Proceedings of the National Academy of Sciences of the United States of America (PNAS) 2005, 102, 315 ; E. Gazit, The FASEB Journal 2002, 16, 77; F. T. Senguen, T. M. Doran, E. A. Anderson, B. L. Nilsson, Molecular BioSystems 2011, 7, 497; F. T. Senguen, N. R. Lee, X. Gu, D. M. Ryan, T. M. Doran, E. A. Anderson, B. L. Nilsson, Molecular BioSystems 2011, 7, 486; I. W. Hamley, Angewandte Chemie International Edition 2007, 46, 8128.

[13] S. S.-S. Wang, Y.-T. Chen, S.-W. Chou, Biochimica et Biophysica Acta 2005, 1741, 307

[14] D. Verbeken, S. Dierckx, K. Dewettinck, Applied Microbiology and Biotechnology 2003, 63, 10

[15] R.C.Randall, G.O.Phillips, P. A. Williams, Food Hydrocolloids 1989, 3, 65

[16] T. Mahendran, P. A. Williams, G. O. Phillips, S. Al-Assaf, T. C. Baldwin, Journal of Agricultural and Food Chemistry 2008, 56, 9269

[17] L. J. Goodruma, A. Patel, J. F. Leykam, M. J. Kieliszewski, Phytochemistry 2000, 54, 99 ; P. A. W. T. Mahendran, G. O. Phillips, S. Al-Assaf and T. C. Baldwin, Journal of Acricultural and Food Chemistry 2008, 56, 9269

[18] M. L. Jayme, D. E. Dunstan, M. L. Gee, Food Hydrocolloids 1999, 13, 459

[19] F. E. Dische, C. Wernstedt, G. T. Westermark, P. Westermark, M. B. Pepys, J. A. Rennie, S. G. Gilbey, R. J. Watkins, Diabetologia 1988, 31, 158

[20] B. Vestergaard, M. Groenning, M. Roessle, J. S. Kastrup, M. v. d. Weert, J. M. Flink, S. Frokjaer, M. Gajhede, D. I. Svergun, PLOS Biology 2007, 5, 1089

[21] M. B. Pepys, P. N. Hawkins, D. R. Booth, D. M. Vigushin, G. A. Tennent, A. K. Soutar, N. Totty, O.Nguyen, C. C. F. Blake, C. J. Terry, T. G. Feest, A. M. Zalin, J. J. Hsuan, Nature 1993, 362, 553

[22] E. S. Voropai, M. P. Samtsov, K. N. Kaplevskii, A. A. Maskevich, V. I. Stepuro, O. I. Povarova, I. M. Kuznetsova, K. K. Turoverov, A. L. Fink, V. N. Uverskii, Journal of Applied Spectroscopy 2003, 70, 868

[23] S. G. Bolder, L. M. C. Sagis, P. Venema, E. v. d. Linden, Langmuir 2007, 23, 4144.
[24] M. Groenning, Journal of Chemical Biology 2010, 3, 1
[25] L. Whitmore, B. A. Wallace, Biopolymers 2008, 89, 392 ; N. Sreerama, R. W. Woody, Analytical Biochemistry 2000, 287, 252
[26] R. R. Porter, Biochemistry journal 1953, 53, 320
[27] L. N. Arnaudov, R. d. Vries, Biophysical Journal 2005, 88, 515
[28] D. J. Tew, S. P. Bottomley, D. P. Smith, G. D. Ciccotosto, J. Babon, M. G. Hinds, C. L. Masters, R. Cappai, K. J. Barnham, Biophysical Journal 2008, 97, 2752
[29] D. M. W. Anderson, J. F. Stoddart, Carbohydrate Polymers 1966, 2, 104
[30] W. Qi, C. Fong, D. T. A. Lamport, Plant Physiology 1991, 96, 848
[31] I. B. Bekard, D. E. Dunstan, Biophysical Journal 2009, 97, 2521
[32] M. Groenning, M. Norrman, J. M. Flink, M. v. d. Weert, J. T. Bukrinsky, G. Schluckebier, S. Frokjaer, Journal of Structural Biology 2007, 159, 483
[33] C. M. Dobson, Nature 2003, 426, 884.
[34] F. Chiti, P. Webster, N. Taddei, A. Clark, M. S. G. Ramponi, C. M. Dobson, Proceedings of the National Academy of Sciences of the United States of America (PNAS) 1999, 96, 3590
[35] R. Khurana, C. Coleman, C. Ionescu-Zanetti, S. A. Carter, V. Krishna, R. K. Grover, R. Roy, S. Singh, Journal of Structural Biology 2005, 151, 229
[36] M. R. H. Krebs, E. H. C. Bromley, A. M. Donald, Journal of Structural Biology 2005, 149, 30.